^{13}C NMR Chemical Shift of Single-Wall Carbon Nanotubes

Sylvain Latil,[1] Luc Henrard,[2] Christophe Goze Bac,[1] Patrick Bernier,[1] and Angel Rubio[3]

[1]*Groupe de Dynamique des Phases Condensées, CNRS-Université de Montpellier 2, France*
[2]*Laboratoire de Physique du Solide, Facultés Universitaires Notre-Dame de la Paix, Namur, Belgium*
[3]*Donostia International Physics Center (DIPC) and Centro Mixto CSIC-UPV/EHU, 20018 San Sebastián/Donostia, Basque Country, Spain*

(Received 8 August 2000)

We compute the magnetic shielding tensor within the London approximation and estimate the Knight shift of single-wall carbon nanotubes. Our results indicate that high resolution ^{13}C NMR should be able to separate the metallic and insulator character of the nanotubes since a 11 ppm splitting is predicted from the respective resonances. As a model for disorder, bending, and defects in these structures, we investigate the magnetic response of nanotubes with finite size. We get a small line broadening coming from an intrinsic length dependent resonance effect. The nanotube packing is also studied and leads to a 20 ppm broadening which disappears under experimental high-resolution conditions.

DOI: 10.1103/PhysRevLett.86.3160 PACS numbers: 76.60.Cq, 71.15.Ap, 75.20.–g

Nuclear magnetic resonance (NMR) has been proved to be a useful tool to study the dynamics and electronic structure of fullerene [1] and nanotube [2,3] materials. In spite of this experimental relevance, for a refined characterization of carbon materials, not much theoretical work is available about infinite sp^2-like carbon objects due to the intrinsic diamagnetic divergence in the graphite susceptibility at $T = 0$ K [4]. Moreover, the change of magnetic properties when going to low dimensional graphitic nanostructures is still not well understood. In particular, single-wall carbon nanotubes (SWNTs), which can be seen as long rolled graphene sheets, have attracted a lot of attention as promising materials for nanotechnology applications and composites. These particular quasi-1D structures, with finite-size effects as a one dimensional quantum box [5,6], show interesting correlations between geometry and electronic properties [7]. Of course, the magnetic response is affected by this interplay, as shown in magnetic susceptibility [8] and magnetotransport [9]. In this Letter, we aim to understand the microscopic mechanisms which contribute to the NMR spectra of SWNTs, by performing a detailed theoretical study of the magnetic response of perfect and isolated tubes as a function of temperature.

By measuring the shift of the Larmor frequency of the nuclear spin, NMR in solids gives information about the chemical environment and the metal-like properties of a compound. The NMR shift which represents the perturbation of the applied field due to the electrons consists of a sum of two tensorial contributions: the shielding tensor $\overleftrightarrow{\sigma}$, which is the contribution of orbital electronic magnetism, and the Knight shift $\overleftrightarrow{K}$, which is a Fermi contact effect of electron spin which appears uniquely in metals. The chemical shift anisotropy tensor $\overleftrightarrow{\delta}$ is measured experimentally by comparing to a standard reference as $\overleftrightarrow{\delta} = \overleftrightarrow{\sigma}_{\mathrm{ref}} - \overleftrightarrow{\sigma} + \overleftrightarrow{K}$ [10]. The $\overleftrightarrow{\sigma}$ tensor can be separated in two parts: the London ring-current (RC) contribution ($\overleftrightarrow{\sigma}_{\mathrm{RC}}$) and the Pople correction [11]. The first part is an effect of the *interatomic* electronic current, and the second one is a local *intraatomic* part that can be written as a function of the hybridization of the carbon atom [12].

Whereas the Knight shift (in metallic compounds) and the Pople part are the dominant contribution to the NMR chemical shift in fullerides due to the very different local environment the C atoms see and the larger s character of the corresponding $\pi_\perp$ orbital ($\simeq$0.08 in C_{60}, for example), this is not the case for the nanotubes. A simple geometric analysis of the curvature of the graphene needed to form tubes with diameters close to the experimental value ($R \simeq 0.68$ nm [13]) indicates that the total degree of $sp^2 - sp^3$ rehybridization of the C atom orbitals is rather small and constant. In fact, the s character of the $\pi_\perp$ hybride orbital slightly varies around 5×10^{-3}. Even if the nanotube is bent, the rehybridization of the $\pi_\perp$ is small compared to that of the fullerene structures. Consequently, the Pople part is nearly the same for all the nanotubes, and does not depend either on the chirality or the particular deformation. Moreover, in high-resolution solid state NMR, the orientation of the ^{13}C is averaged with respect to the magnetic field, and only the isotropic part of the chemical shift tensor is measured: $\sigma_{\mathrm{iso}} = \frac{1}{3}\mathrm{Tr}[\overleftrightarrow{\sigma}]$. In our case, the Pople part gives rise to a global shift of the whole magnetic response and will not allow us to distinguish between different tubes. Thus as we are interested in relative changes of the chemical shift tensor we can safely neglect this part in the present calculations [14]. Furthermore, since the density of states of SWNTs at the Fermi level is small, $g(E_f) \simeq 0.015$ states/eV · spin · atom [15], the Knight shift contribution can be neglected in the present study.

SWNTs are usually closely packed in bundles with an average intertube distance of 3.4 Å. Tube-tube interactions might influence the shift of a given ^{13}C spin and, therefore, have to be considered. To make direct contact with experiments, it is also important to look at the modification of the properties of perfect structures induced by disorder or defects. Indeed, SWNTs with length of $\sim$1 μm are

 0031-9007/01/86(14)/3160(4)$15.00

never perfectly straight: TEM images show that they are often bent or kinked [16]. Since the local density of states is drastically modified by these defects [17], they can be seen as a set of nearly isolated straight segments of finite length, interconnected by bendings or defects [18]. Similarly, localization centers, such as junctions, Stone-Wales defects, or chemical functionalizations, can affect the magnetic response by creating effective quantum boxes within the tube. We point out that even if the number of those centers is scarce and hard to be directly observed in a NMR experiment, their presence defines a confinement region (quantum box) that drives a change in the magnetic response of the carbon atoms within the quantum box. Hence, bundle and finite-size effects have to be considered when describing experimental NMR studies.

From the previous discussion, we are left with the computation of the London RC part of the shielding tensor $\overleftrightarrow{\sigma}_{\mathrm{RC}}$. This is done by introducing a probe dipole $\mathbf{m}$ in the system (where the ^{13}C spin sits) that interacts with the external applied magnetic field $\mathbf{H}_0$ and the electron-induced magnetic field. The $\overleftrightarrow{\sigma}_{\mathrm{RC}}$ tensor can be defined through the corresponding Zeeman splitting due to the total internal field as $2\mathbf{m}\cdot\mathbf{H} = 2\mathbf{m}\cdot(\overleftrightarrow{1} - \overleftrightarrow{\sigma}_{\mathrm{RC}})\cdot\mathbf{H}_0$. If now we remove the direct interaction between $\mathbf{H}_0$ and $\mathbf{m}$ we get the following expression for the $\overleftrightarrow{\sigma}_{\mathrm{RC}}$ tensor:

$$(\sigma_{\mathrm{RC}})_{\alpha\beta} = \left(\frac{\Omega(\mathbf{H}_0,\mathbf{m},T) - \Omega(\mathbf{H}_0,-\mathbf{m},T)}{2mH_0}\right)_{\mathbf{H}_0\|\alpha,\mathbf{m}\|\beta}, \quad (1)$$

where α and β are the spatial directions x, y, or z (the tube axis is assumed to be along the z direction), Ω is the grand-canonical potential at temperature T defined as

$$\Omega(\mathbf{H}_0,\mathbf{m},T) = -k_BT\sum_n \ln\left[1 + \exp\left(\frac{\epsilon_F - \epsilon_n}{k_BT}\right)\right]. \quad (2)$$

Here ϵ_n are the eigenenergies of the system under the action of the applied field $\mathbf{H}_0$ and the dipole moment $\mathbf{m}$, and ϵ_F is the Fermi level. Briefly, we use a tight-binding model with one π electron per site and expand the secular equation on a gauge-invariant basis set. The field-dependent hopping t_{ij} between two atomic orbitals i and j is taken as the free hopping t_{ij}^0 multiplied by a phase factor [19,20]:

$$t_{ij} = t_{ij}^0 \exp\left(\frac{-ie}{2\hbar c}(\mathbf{A}_i - \mathbf{A}_j)\cdot(\mathbf{R}_i + \mathbf{R}_j)\right) \quad (3)$$

with $\mathbf{R}_i$ the position of site i, and $\mathbf{A}_i = \mathbf{A}(\mathbf{R}_i)$ the vector potential at site i [21]. The RC shielding tensor is diagonalized and from the three principal values the static line shape of the NMR powder spectrum is obtained [22]. In our case, the σ_{zz} component is a principal value of the tensor, as a consequence of the uniaxial character of the nanotube. The two other components are called the radial σ_{rad} and orthoradial σ_{ortho}.

Figure 1 presents the computed powder spectra of RC chemical shift tensor for isolated infinite nanotubes at room temperature. We find a very weak dependence of the line shape on both tube radius and chirality. Only the σ_{zz} component is different according to the metallic or semiconducting character of the tube. For clarity, only the $(10,10)$ metallic and the semiconductor $(12,8)$ tubes are drawn. The σ_{zz} principal value is T independent and diamagnetically shifted for semiconductors. For metallic tubes, it is paramagnetically shifted, with a $1/T$ dependence as shown in the inset. The σ_{rad} and σ_{ortho} values are always diamagnetic, but σ_{ortho} is much smaller than σ_{rad}. Therefore NMR can resolve the electronic tube character but not the underlying structural properties of carbon nanotubes.

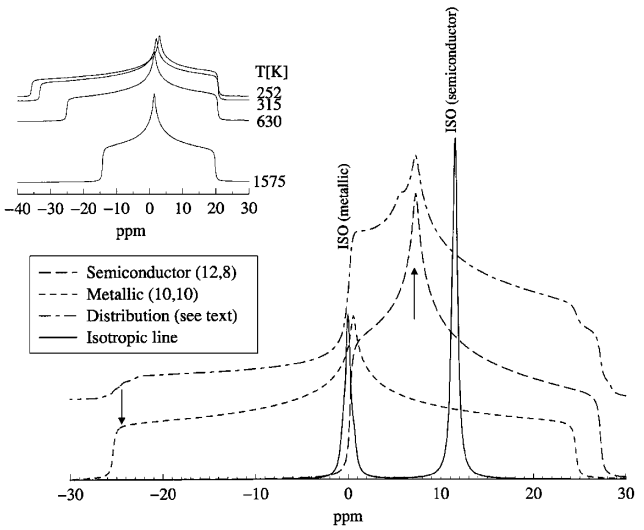

FIG. 1. Calculated $\overleftrightarrow{\sigma}_{\mathrm{RC}}$ tensor for infinite, isolated, and perfect SWNTs. They illustrate the distinct magnetic response depending on the specific electronic character of the tube: the σ_{zz} principal value (shown with arrows) is paramagnetic ($\sigma_{zz} < 0$) for a metallic tube and diamagnetic ($\sigma_{zz} > 0$) for a semiconductor. The $1/T$ temperature dependence of the σ_{zz} element of metallic tube shielding tensor is shown in the inset [the given example is the $(5,5)$ tube]. The simulated response of a bulk sample (see text) is shown as a distribution of static tensors, or isotropic lines, where the response of metallic and semiconducting tubes is separated by 11 ppm.

As tube chirality cannot be selected in the production process, we also performed a random distribution that will simulate an actual sample in the diameter range determined experimentally [13]. We fixed the ratio of the numbers of metallic and semiconducting tubes to 1 to 2. The static response is drawn in Fig. 1; however, the most relevant result is the isotropic line of the sample where a splitting of 11 ppm between the metallic and semiconducting response is predicted. The metallic line is found to be near zero, whereas the semiconducting one is diamagnetically shifted. This splitting and the relative intensities of the lines could be used to probe the metallic-insulator ratio in bulk sample with high-resolution NMR measurements.

It is important to check how the properties of these isolated structures are changed when they are packed into a bundle. We use two approximations: first, the tube-tube interactions are neglected, then the bundle is considered as

a set of isolated structures. With this assumption, the total field acting on the ^{13}C is the sum of the applied field and the contributions of each tube:

$$\mathbf{H} = \left(\overleftrightarrow{\mathbf{1}} - \sum_{i\in\text{bundle}} \overleftrightarrow{\sigma}^{(i)}\right)\mathbf{H}_0 . \quad (4)$$

Second, we keep only first-nearest-neighbor interaction, as

$$\mathbf{H} = (\overleftrightarrow{\mathbf{1}} - \overleftrightarrow{\sigma}^{(1)} - \overleftrightarrow{\sigma}^{(2)})\mathbf{H}_0 , \quad (5)$$

where $\overleftrightarrow{\sigma}^{(1)}$ is the internal chemical shift of the tube carrying the nuclear magnetic moment $\mathbf{m}$ (result shown in Fig. 1), and $\overleftrightarrow{\sigma}^{(2)}$ is the shift due to the tube which is located at approximately 3.4 Å from the ^{13}C. Since the magnetic interaction is not sensitive upon the chirality, and the radius is basically constant in a bundle, we restricted our model to the metallic $(10, 10)$ and semiconducting $(12, 8)$ which have equivalent radii. A 20 ppm broadening of the tensor due to the influence of the first neighbor tube is obtained. It is of the same order of magnitude as the metallic-semiconductor splitting. Hence the static shielding tensor $\overleftrightarrow{\sigma}_{\text{RC}}$ for isolated tubes is no longer relevant. However, our results indicate that the $\overleftrightarrow{\sigma}^{(2)}$ tensor is quasi-independent of the electronic properties of the first neighbor tube. In addition, this tensor is symmetric and centered at 0 ppm, then it reduces to a Lorentzian centered near zero $\sigma^{(2)}_{\text{iso}} \simeq 0$, when averaged over all orientations. The isotropic average of all the bundle will be nearly equal to the isotropic value of the isolated tube,

$$\left(\sum_{i\in\text{bundle}} \overleftrightarrow{\sigma}^{(i)}\right)_{\text{iso}} \simeq \sigma^{(1)}_{\text{iso}} , \quad (6)$$

and the problem of broadening is circumvented.

We turn now to the calculation of the effects of disorder and bendings treated as finite-size effects. The resonant behavior in armchair tubes which appears as a closing of the highest occupied–lowest unoccupied molecular orbital (HOMO-LUMO) gap each time the length of the box is $3n + 1$ periods has already been predicted [23,24]. These "magic numbers" can be explained by a simple particle-in-a-box model [5], and are found to be an important criterion in tunneling magnetic transport [25]. It is worth noting that not only armchair tubes, but also some chiral ones show this resonant behavior, such as the $(11, 2)$ or the $(7, 4)$, for example. It is possible to write a criterion to determine if the tube will be resonant or not [26]. We show in Fig. 2a that the static susceptibility (case $\mathbf{H}_0 \parallel z$) of the finite $(5, 5)$ armchair tube is maximum for $L = 1.23 + n \times 7.38$ Å. That corresponds to $(n + \frac{1}{2})\lambda_F$ and to the closing of the HOMO-LUMO gap of the structure. This property is consistent with Van Vleck paramagnetism, where the effect of the magnetic field is written as a second order perturbation, which is divergent when the Fermi level is degenerate. The resonant behavior (magic numbers) of the $(11, 2)$ is also presented. We show on the same figure that none of the zigzag tubes [we take the $(10, 0)$ and $(9, 0)$ as examples] exhibit resonances as a consequence of the same criterion [26]. To illustrate the microscopic phenomena acting in the magnetic response of small systems, we plot in Fig. 3 the interatomic currents, due to an applied field ($\mathbf{H}_0 \parallel z$), on the $(10, 10)$ tube with two different lengths. These currents are localized at the antinodes of the standing waves along the 1D box, and reach a maximum when the interference is constructive, i.e., when the length is $3n + 1$ periods. By comparison, nonresonant tubes such as the $(9, 0)$ show a uniform distribution of currents, without the $\lambda_F/2$ oscillations.

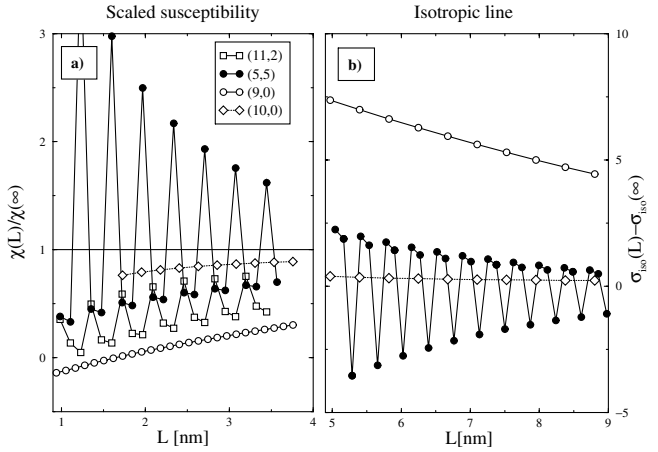

FIG. 2. Finite length effects in magnetic response of carbon nanotubes. (a) The scaled magnetic susceptibility $\chi(L)/\chi(\infty)$ for different finite-size tubes when $\mathbf{H}_0 \parallel z$. The "magic numbers" in the response of armchair $(5, 5)$ or chiral $(11, 2)$ are visible with a $\lambda_F/2$ periodicity, whereas the evolution of the susceptibility for semiconducting or nonresonant metallic tubes such as zigzag tubes is continuous. (b) The magic numbers are still present in the isotropic line σ_{iso} of armchair tubes. By comparison, nonresonant tubes show a smooth evolution of the σ_{iso}. Semiconducting tubes reach the value of infinite tube very early and do not show any finite length effect.

We check how the magnetic response of tube elements with length L affects the isotropic line of the shielding tensor, by plotting on Fig. 2b, the difference $\sigma_{\text{iso}}(L) - \sigma_{\text{iso}}(\infty)$. The ^{13}C spin is located in the bulk of the tube to avoid the edges' effects. The response of a finite-size structure differs from the response of an infinite tube mainly by the σ_{zz} element for the metallic tubes. The broadening of the linewidth, due to the distribution of lengths, acts uniquely on the line of the metallic tubes. This broadening exhibits a $1/L$ dependence (see Fig. 2b). For realistic lengths between two scattering centers ($\simeq$0.1 μm) this broadening appears to be very small ($<$0.5 ppm).

In summary, we have performed a systematic study of the ^{13}C NMR chemical shifts of SWNTs. We have shown that the Knight shift and the *intraatomic* part of the orbital contribution can be removed without losing the physical relevance of the computations. The ring currents' contribution to the NMR shift of perfect and isolated SWNTs shows a 11 ppm splitting between the isotropic lines of semiconducting and metallic nanotubes. This distinct

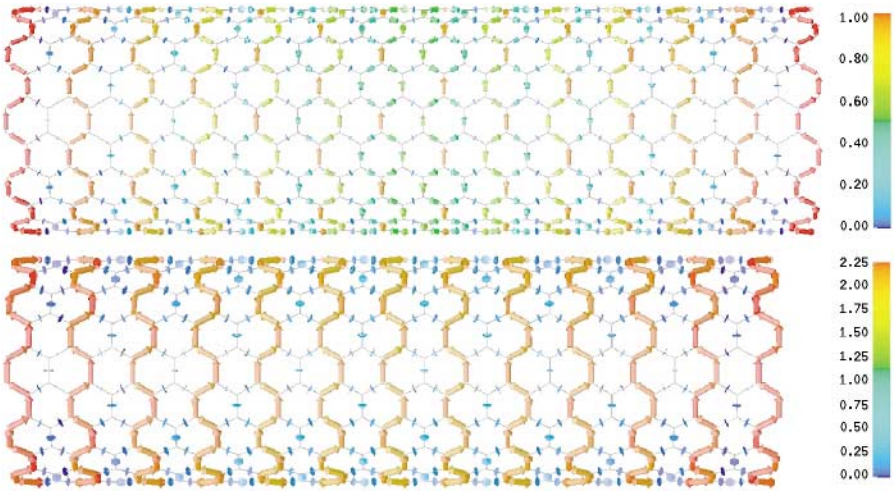

FIG. 3 (color). Interatomic currents for a finite metallic $(10, 10)$ tube. The results are in units of $\mathbf{J}_{\text{benzene}}$. Bottom: Tube with a length of 19 unit cells (magic number) where the $\lambda_F/2$ oscillations are visible, with a weak localization at the edges. Top: Tube with a length of 20 unit cells (nonmagic number), where the currents are lower and show destructive interferences in the middle of the box.

response could be used to characterize the electronic structure of a bulk nanotube sample. In addition, we prove that this splitting is still relevant even if the bundle packing of tubes and the finite-size effects are taken into account. Finally, the presence of paramagnetic or ferromagnetic impurities in the vicinity of bundles (that actually happens in experiments) will broaden the NMR response due to the inhomogeneous local field created by these impurities that act on the ^{13}C sites [27].

Financial support was given by the European Community through its TMR programmes and by JCyL (VA28/99). L. H. was supported by FNRS and the PAI 4/10 project. The computer facilities of CINES (Montpellier) and especially M. Falandry are acknowledged.

[1] R. Tycko *et al.,* J. Chem. Phys. **99**, 7554 (1993).
[2] X.-P. Tang *et al.,* Science **288**, 492 (2000).
[3] C. Goze Bac *et al.,* Phys. Rev. B (to be published).
[4] J. W. McClure, Phys. Rev. **119**, 606 (1960).
[5] A. Rubio *et al.,* Phys. Rev. Lett. **82**, 3520 (1999).
[6] L. C. Venema *et al.,* Science **283**, 52 (1999).
[7] J. Mintmire, B. Dunlap, and C. White, Phys. Rev. Lett. **68**, 631 (1992).
[8] J.-P. Lu, Phys. Rev. Lett. **74**, 1123 (1995); the susceptibility of infinite and isolated tubes when $\mathbf{H}_0 \parallel z$ is diamagnetic for semiconducting tubes and paramagnetic for metallic tubes. When $\mathbf{H}_0 \perp z$, it is diamagnetic in any case.
[9] R. Saito, G. Dresselhaus, and M. Dresselhaus, *Physical Properties of Carbon Nanotubes* (Imperial College Press, London, 1998).
[10] Tetramethylsilane is usually taken as reference. Since we are not interested in absolute but in relative shifts in this work, we will take $\sigma_{\text{ref}} = 0$.
[11] J. Pople, J. Chem. Phys. **37**, 53 (1962).
[12] A. Pasquarello, M. Schlüter, and R. C. Haddon, Phys. Rev. A **47**, 1783 (1993).
[13] S. Rols *et al.,* Eur. Phys. J. **10**, 263 (1999).
[14] For the present work this approximation is reasonable. However, a more refined first-principles approach would be required to include the effects of impurities, chemical functionalization, and doping in nanotubes. See F. Mauri *et al.,* Phys. Rev. Lett. **79**, 2340 (1997), and references therein for the method applied to carbon materials.
[15] J. Mintmire and C. White, Phys. Rev. Lett. **81**, 2506 (1998).
[16] C. Journet *et al.,* Nature (London) **388**, 756 (1997).
[17] A. Rochefort, D. R. Salahub, and P. Avouris, Chem. Phys. Lett. **297**, 45 (1998).
[18] A. Bezryadin *et al.,* Phys. Rev. Lett. **80**, 4036 (1998).
[19] L. Salem, *The Molecular Orbital Theory of Conjugated Systems* (W. A. Benjamin Inc., Reading, 1966); see Chap. 4 (pp. 189–223).
[20] We take the value of the hopping $t_{ij} = 2.7$ eV. We know that different values have been proposed, but the exact value does not influence the present results much.
[21] We have $\mathbf{A} = \mathbf{A}^{\text{H}_0} + \mathbf{A}^m$, where $\mathbf{A}^m(\mathbf{r}) = \mathbf{m} \times \mathbf{r}/r^3$. The London method implies that $\nabla \cdot \mathbf{A} = 0$, and for an infinite tube, the Bloch theorem remains valid only if the matrix elements satisfy the z translational symmetry, the chosen gauge is then $A_x^{\text{H}_0} = B_y z - \frac{1}{2} B_z y$, $A_y^{\text{H}_0} = -B_x z + \frac{1}{2} B_z x$, and $A_z^{\text{H}_0} = 0$.
[22] M. Mehring, *High Resolution NMR in Solids* (Springer-Verlag, Heidelberg, 1976), Chap. 2.4.
[23] H.-Y. Zhu *et al.,* J. Phys. Chem. Solids **59**, 417 (1998).
[24] A. Rochefort, D. R. Salahub, and P. Avouris, J. Phys. Chem. B **103**, 641 (1999).
[25] H. Mehrez *et al.,* Phys. Rev. Lett. **84**, 2682 (2000).
[26] The criterion to have a resonant (n, m) tube is $n - m$ is a multiple of $3d$, where d is the greatest common divisor of n and m. Further details will be given elsewhere.
[27] Similar effects would be present when studying the filling of tubes with transition metal atoms [C. Guerret-Plécourt *et al.,* Nature (London) **372**, 761 (1994)].